Isotropic-nematic phase transition in athermal solutions of rod-coil diblock copolymers

Tao Jiang and Jianzhong Wu[a)]
Department of Chemical and Environmental Engineering, University of California, Riverside, California 92521

(Received 14 March 2007; accepted 30 May 2007; published online 17 July 2007)

We present a hybrid method to investigate the isotropic-nematic (I-N) transition in athermal solutions of rod-coil copolymers. This method incorporates the scaled-particle theory for semiflexible chains with two-chain Monte Carlo simulation for the osmotic second virial coefficient and for the angle-dependent excluded volume. We compare the theoretical prediction with Monte Carlo simulations for fused rod-coil copolymers and find good agreement for both the equation of state and the orientational order parameter. The theory is also used to examine the effects of the bond length, the chain length, and the chain composition on orientational ordering in athermal solutions of rod-coil block copolymers. It predicts I-N transition in rod-coil copolymers with fixed rod length but a variable flexible tail in good agreement with experiments. © *2007 American Institute of Physics*. [DOI: 10.1063/1.2751497]

I. INTRODUCTION

In a pioneering work published in 1949,[1] Onsager demonstrated that the excluded-volume effect is sufficient to induce the isotropic-nematic phase transition in a lyotropic liquid crystal. Onsager's theory agrees well with experiments for systems containing long rodlike molecules such as the colloidal dispersions of the tobacco mosaic virus.[2] However, it is accurate only at the level of the osmotic second virial coefficient. For systems where higher-order virial coefficients are significant, Onsager's theory underpredicts the excluded-volume effects and may yield an unphysical packing density at the isotropic-nematic transition. Aiming toward a more faithful description of the isotropic-nematic phase transition has generated a rich literature of liquid-crystal theories including the Flory theory,[3] Khokhlov-Semenov theory,[4,5] Parsons-Lee theory,[6–8] and more recently, various versions of the density functional theory.[9–14] These theoretical efforts have also inspired a number of molecular simulations for various phase transitions in liquid-crystalline systems.[15–19] The molecular models for describing lyotropic liquid crystals have been extended from hard rods to hard spherocylinders,[7,8] hard ellipsoids,[15] linear tangent[10,16] or fused[13] sphere chains, semiflexible tangent[11,17] or fused sphere chains,[12] and most recently rod-coil sphere chains.[18,19] While later versions of the liquid-crystal theories provide a more faithful description of the excluded-volume effects, they are often compromised by a mean-field description of the osmotic second virial coefficient.

In recent years block copolymers made of rigid and flexible components have received a great deal of research interest for their ability to self-assemble into a variety of nanostructures.[20–28] Many functional polymers of practical interest belong to this category, such as nonfluorous CO_2-philic polymers,[29] conjugated polymers,[30] and certain polypeptides.[31] Possible microphases in rod-coil copolymers include micelles, isotropic, lamellar, nematic, and various smectic phases.[32–34] While some of these phases are similar to those appearing in a conventional liquid crystal, qualitative differences are expected due to introduction of the flexible tail. Recently, Chochos *et al.* noted that the coil block may have significant effect on the properties of rod-coil diblock copolymers in thin films.[35]

Previous theoretical investigations of rod-coil copolymers are based primarily on the polymer self-consistent-field theory[32–34] (SCFT) or on molecular simulations.[18,19,36,37] For example, Duchs and Sullivan obtained a phase diagram for the dilute solutions of wormlike diblock copolymers and found that the nematic-smectic transition is of second order.[33] The SCFT was also employed to investigate the phase behavior of rod-coil block copolymer melts and the influences of temperature and composition on the microscopic structure.[32–34] On the other hand, McBride and Wilson[36] employed molecular simulations to study a model system consisting of a Gay-Berne core and two flexible alkyl chains at both sides (C_3–GB–C_7). A nematic phase was identified at high packing density. Due to the heavy computational cost, the atomic simulation method becomes inefficient for studying phase transitions in rod-coil block copolymers. On the other hand, simulations based on coarse-grained models have been reported by van Duijneveldt and Allen[37] and by McBride *et al.*[18,19] It was found that the flexible block in general hinders formation of the nematic phase but stabilizes smectic phases. Because the ordered phases typically appear at high packing density, computation of the phase transition is challenging even within the simplified models. Indeed, published simulation results are often limited to short-chain representation of liquid-crystal molecules.[18]

In recent years, a number of equations of state have been proposed to predict phase transitions in lyotropic liquid crys-

[a)]Electronic mail: jwu@engr.ucr.edu

tals, in particular, for the isotropic-nematic transition within the framework of the hard-sphere-chain models.[10–13,38,39] In general, these equations of state are computationally much more efficient in comparison with either SCFT or molecular simulations. Two analytical approaches are particularly useful in deriving the equation of state: One is based on the first-order thermodynamic perturbation theory (TPT1) and the other is based on the scaled-particle theory (SPT). Extension of TPT1 to liquid-crystal systems relies on a rescaling method first introduced by Parsons,[6] Lee,[7] and Lee and Meyer.[8] According to this method, the thermodynamic properties of an ordered phase can be obtained by rescaling the corresponding properties of the isotropic phase with the osmotic second virial coefficients. Despite its simplicity, predictions from the semiempirical rescaling method are often found satisfactory in comparison with simulations and with experiments.[10,38] Unlike TPT1, SPT avoids the semiempirical rescaling and is directly applicable to various liquid-crystal phases.[40–45] However, it requires an input for the osmotic second virial coefficient and for the ordered phases, the orientation-dependent excluded volume of anisotropic molecules.

While both TPT1 and SPT are quite accurate at high packing densities, they are less satisfactory for semiflexible chains at dilute or semidilute regimes. Indeed, neither TPT1 nor SPT gives the correct osmotic second virial coefficient for semiflexible chains. In this work, we introduce a hybrid method that incorporates SPT with two-chain Monte Carlo simulation for the osmotic second virial coefficient and for the orientation-dependent excluded volume. Different from alternative equations of state for semiflexible chains, the hybrid method is accurate at both low and high packing densities and is directly applicable to the nematic phase and to molecules of arbitrary topology.[46]

In Sec. II, we describe the theoretical details of the hybrid method. Section III proceeds to compare with simulation results for the osmotic pressure and structural ordering in athermal solutions of fused rod-coil chains. Also discussed in Sec. III are the theoretical predictions for the effects of the bond length and the chain flexibility on the isotropic-nematic transition. Section IV summarizes the main results and conclusions.

II. THEORY AND MOLECULAR MODEL

A. Molecular model

The rod-coil copolymer studied in this work consists of a rigid block of m_r hard spheres and a flexible block of m_f hard spheres of the same kind connected in a linear configuration; the total chain length is $m=m_r+m_f$. The theory is applicable to both fused chains and to tangent chains. For systems considered in this work, the bond length is in the range of $L=0.6\sigma-\sigma$, where σ is the hard-sphere diameter. For the rigid block, the hard spheres are connected in a rodlike configuration; for the flexible block, the hard spheres are connected with a fixed bond length but fully flexible bond angles. The interaction between any nonbonded particles is represented by the hard-sphere potential. The same model has been used in earlier Monte Carlo simulations for rigid-flexible copolymers.[18,19]

B. Scaled-particle theory

The Helmholtz free energy for the model system can be represented by an ideal part and an excess

$$\frac{\beta F}{N}=\ln(\Lambda^3\rho)-1+\int f(\Omega)\ln[4\pi f(\Omega)]d\Omega+\frac{\beta F^{\mathrm{ex}}}{N}, \quad (1)$$

where N is the number of molecules (chains), ρ is the molecular number density, Λ is the thermal wavelength, and $\beta=1/k_BT$ with k_B being the Boltzmann constant and T the absolute temperature. The Euler angle Ω represents a molecular orientation that will be discussed in more detail later, and $f(\Omega)$ is the orientational distribution function. The first two terms on the right side of Eq. (1) correspond to the ideal-gas contribution; it arises from the translational and rotational freedoms of anisotropic molecules; the last term represents the excess Helmholtz energy due to the molecular excluded volume.

While the SPT was originally derived for rigid convex particles, it has been extended to athermal models of flexible or semiflexible polymers. According to Boublik *et al.*[41] and Cotter,[44] the excess Helmholtz energy for an athermal polymeric system is given by

$$\frac{\beta F^{\mathrm{ex}}}{N}=(\psi-1)\ln(1-\eta)+\frac{3\alpha\eta}{(1-\eta)}+\frac{\psi\eta}{(1-\eta)^2}, \quad (2)$$

where $\eta=\rho\nu$ is the packing fraction and ν is the molecular volume. The nonsphericity parameter α is determined from the reduced second virial coefficient $B_2^*=B_2/\nu$:

$$\alpha=\frac{B_2^*-1}{3}. \quad (3)$$

The parameter ψ is given by[12]

$$\psi=\frac{\sigma s}{9\nu}\left[3\alpha-\left(\frac{\sigma s}{4\nu}\right)\left(1-(m-1)\left(\frac{L}{2\sigma}\right)^2\right)\right], \quad (4)$$

where m and s stand for the chain length and the molecular surface area, respectively. For a fused chain of spherical particles, the molecular volume and surface area are given by

$$\nu=\frac{\pi\sigma^3}{6}\left\{1+\frac{1}{2}(m-1)\left[\frac{3L}{\sigma}-\left(\frac{L}{\sigma}\right)^3\right]\right\}, \quad (5)$$

$$s=\pi\sigma^2\left[1+(m-1)\frac{L}{\sigma}\right]. \quad (6)$$

Except for B_2^*, all parameters can be directly evaluated from the molecular models. An essential task in the application of SPT is thus to determine B_2^*. In an earlier work,[12,13] B_2^* is determined by a semiempirical correlation.

Based on the Helmholtz energy, we can readily derive the equation of state and other pertinent thermodynamic properties. For example, the orientational entropy is calculated from the angle-distribution function

$$\frac{S_{or}}{Nk_B} = -\int f(\Omega)\ln[4\pi f(\Omega)]d\Omega. \tag{7}$$

The packing entropy or entropy due to the excluded-volume effect is given by

$$\frac{S_{pa}}{Nk_B} = -\frac{\beta F_{ex}}{N}. \tag{8}$$

C. Osmotic second virial coefficient

In an athermal solution of semiflexible chains, the osmotic second virial coefficient is given by

$$B_2 = \tfrac{1}{2}\int\int d\{\mathbf{\Omega}\}d\{\mathbf{\Omega}'\}f(\{\mathbf{\Omega}\})f(\{\mathbf{\Omega}'\})V_{ex}(\{\mathbf{\Omega}\},\{\mathbf{\Omega}'\}), \tag{9}$$

where $V_{ex}(\{\mathbf{\Omega}\},\{\mathbf{\Omega}'\})$ represents the excluded volume of two chains with conformations $\{\mathbf{\Omega}\}$ and $\{\mathbf{\Omega}'\}$; $\{\}$ denotes the ensemble of molecular configurations for a single chain. Because of the chain flexibility, the chain orientation cannot be represented by a unit vector as for a rigid rod. The dynamic nature of intramolecular configurations makes evaluation of B_2 rather complicated. In an earlier application of SPT, Jaffer *et al.*[12] assumed that the osmotic second virial coefficient of semiflexible chains can be equivalently represented by those for a binary mixture of hard spheres and hard dimers. In that case, a molecular orientation matrix can be used to describe the orientation vectors of all the diatomic molecules. In the nematic phase, the orientational distribution function $f(\{\mathbf{\Omega}\})$ is solved by integration of all possible chain conformations, which can be done by using a Monte Carlo simulation method. Because of the uniform orientational distribution, this method generates a second virial coefficient B_2 identical for rigid and semiflexible chains in the isotropic phase. The hard-dimer approximation is valid only for relatively short chains.[41] For long chains, B_2 depends strongly on the chain flexibility even in the isotropic phase.[18]

In this work, we evaluate B_2 by using a two-chain Monte Carlo simulation method first proposed by Fynewever and Yethiraj.[11] According to this method, the molecular orientation ensemble $\{\mathbf{\Omega}\}$ is described by the orientation of the overall molecular axis defined by the eigenvector corresponding to the smallest eigenvalue of the molecular moment of inertia tensor, Ω. In terms of the Euler angle of the molecular axis Ω, the expression for B_2 is reduced to

$$B_2 = \tfrac{1}{2}\int\int d\mathbf{\Omega}d\mathbf{\Omega}'f(\mathbf{\Omega})f(\mathbf{\Omega}')V_{ex}(\mathbf{\Omega},\mathbf{\Omega}'), \tag{10}$$

where $V_{ex}(\mathbf{\Omega},\mathbf{\Omega}')$ is the excluded volume for two chains with fixed intermolecular orientations. To calculate $V_{ex}(\mathbf{\Omega},\mathbf{\Omega}')$, we first generate a large number of chain configurations $(m=m_r+m_f)$ by the recoil-growth algorithm and 100 pairs are selected for sampling the two-body interactions. For each pair, the center of one chain is fixed at the center of the simulation box and the second chain is rotated to a fixed relative angle $\gamma=\Omega-\Omega'$. Monte Carlo simulation is applied to 100 000 random translational moves of the second chain. This procedure is repeated for all 100 pairs of the semiflexible chains with different initial configurations. The excluded volume is calculated from

$$\nu_{ex}(\gamma) = \frac{N_{overlap}}{N_{total}}\nu_{box}, \tag{11}$$

where N_{total} and $N_{overlap}$ are, respectively, the number of the total moves and the number of those leading an overlap and ν_{box} is the volume of the simulation box. As discussed in Ref. 11 we only calculate seven relative angles equally distributed from 0 to $\pi/2$. The excluded volumes at other angles are calculated by a polynomial interpolation.[47] We have tested the interpolated results by comparing with the exact values from simulations. The interpolation method introduces no noticeable deviations but significantly improves the computational efficiency.

D. Phase transition calculations

At a given packing fraction, we determine the orientational distribution function $f(\mathbf{\Omega})$ by minimizing the Helmholtz energy,

$$\frac{\delta F[f(\Omega)]}{\delta f(\Omega)} = 0, \tag{12}$$

subjected to the normalization condition

$$\int f(\Omega)d\Omega = 1. \tag{13}$$

Equations (12) and (13) can be solved by using an iterative method.[48]

To compute the densities or packing fractions of the coexisting isotropic and nematic phases, we solve the minimization problem in combination with the conditions of the phase equilibrium:

$$\beta p^{iso} = \beta p^{nem}, \qquad \beta\mu^{iso} = \beta\mu^{nem}, \tag{14}$$

where μ is the chemical potential, p is the osmotic pressure, and the superscripts iso and nem represent the isotropic and nematic phases, respectively. Both the osmotic pressure and chemical potential can be readily derived by differentiations of the Helmholtz energy.

III. RESULTS AND DISCUSSION

A. Comparison with simulations

We first calibrate the numerical performance of the hybrid method by comparison with molecular simulations. McBride *et al.*[18,19] studied the isotropic (I)-nematic (N) phase transition of rod-coil diblock copolymers using Monte Carlo simulations. They employed a fused-chain model with the bond length $L=0.6\sigma$ and total chain length $m=15$. By changing the composition of the rigid and flexible blocks, they studied the influence of intramolecular flexibility on the I-N phase transition. For direct comparison, the same model is used in our theoretical calculations.

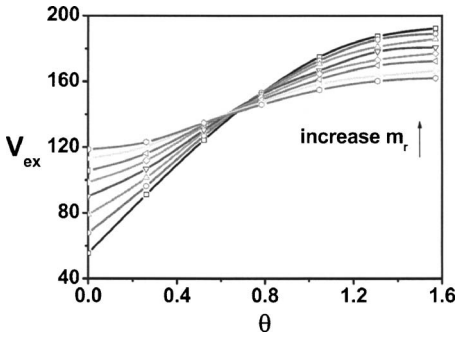

FIG. 1. The angular dependence of the excluded volumes for rod-coil copolymers ($m=15$, $L=0.6\sigma$) obtained from two-chain Monte Carlo simulation. The lines represent different chain compositions with $m_r=15$, 14, 13, 12, 11, 10, 9, and 8.

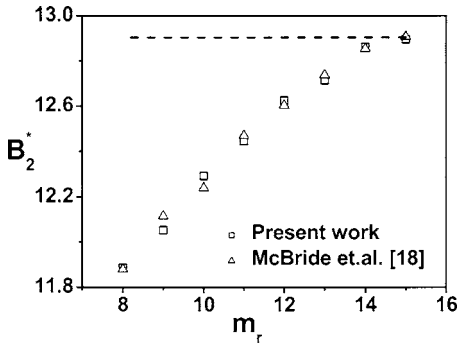

FIG. 2. The reduced osmotic second virial coefficients ($B_2^*=B_2/\nu$) for the systems shown in Fig. 1. The squares are results from the present work and the triangles are from Mcbride *et al.* (Ref. 18). The dashed line corresponds to the analytical results from Jaffer *et al.* (Refs. 12 and 13).

Figure 1 shows the angle dependence of the excluded volume for the rod-coil copolymers with the number of segments in the rigid block changing from $m_r=8$ to 15. We observe that for each case considered here, the excluded volume at parallel configuration is smaller than that at perpendicular configuration. The monotonic increase of the exclude volume with angle can be understood from the semiflexible nature of copolymers.[11,49] As m_r increases, the chain contracts in the direction perpendicular to the molecular axis and stretches along the molecular axis. For $m_r=15$, the chain becomes totally rigid and the difference in the excluded volume between parallel and perpendicular orientations is the largest.

With the information on the excluded volume, we can calculate B_2^* for the isotropic phase from Eq. (10) by setting $f(\Omega)=1/4\pi$. Figure 2 compares the simulation results from this work with those obtained by McBride *et al.*[18] following an algorithm proposed by Vega.[50] As expected, the different simulation methods yield similar results. We observe that B_2^* declines noticeably as the molecular flexibility increases. The reduction of B_2^* with the chain flexibility can be explained by the decrease of the excluded volume at high interception angles, as shown in Fig. 1. The dashed line in Fig. 2 shows a constant B_2^* predicted by the analytical method proposed by Jaffer *et al.*[12] and by Diplock *et al.*[45] Although the analytical method gives the correct results for rigid chains, it is evident that the approximation is poor for semiflexible chains. Even in the isotropic phase, B_2^* depends on the chain flexibility and its deviation from that corresponding to a rigid chain increases with the chain flexibility. Although the same SPT equations are used by Jaffer *et al.*[12] and by Diplock *et al.*,[45] the current hybrid method is more accurate because it utilizes an exact osmotic second virial coefficient. We expect that the improvement is significant in predicting the thermodynamic properties of semiflexible chains, especially in the isotropic phase.

Next we compare the theoretical predictions for the osmotic pressure and for the I-N transition in rod-coil copolymers with those obtained from molecular simulations. Figure 3 shows the reduced osmotic pressure $P^*=\beta P\nu$ versus the packing fraction for rod-coil copolymers of fixed total length ($m=15$) with the rigid block varying from $m_r=15$, 13, 11, 10, 9, and 8. As defined in Eq. (5), ν is the molecular volume. The solid lines represent theoretical predictions from this work and the symbols are the simulation results from Refs. 18 and 19. In general, the hybrid method finds satisfactory agreement with the simulations, especially for rigid chains with $m_r \geqslant 11$ [shown in Figs. 3(a)–3(c)]. The theory provides a quantitative description of the equation of state for both the isotropic and nematic phases. The deviations at high packing fractions are probably due to the formation of smectic phases, as indicated in the simulation work. In the smectic phase, the rod-coil copolymers possess not only an orientational order but also a positional order. A correct description of the smectic phase would require generalization of the current method for inhomogeneous systems.

While the current theory is very accurate for the isotropic phase, agreement between theory and simulation seems to deteriorate for the nematic phase as the copolymer becomes more flexible. In contrast to Onsager's theory, SPT overpredicts the excluded volume effect, which may result in an I-N phase transition at lower packing density (at the same packing density, the pressure for a nematic phase is lower than that for the isotropic phase). However, it is unlikely that the error increases with the chain flexibility because the accuracy of SPT for flexible chains has been well established.[40–43] As a result, the discrepancy shown in Fig. 3 is likely attributed to the nontrivial simulation of a condensed multiple chain system. Indeed, the theory reproduces the simulation results for rigid chains [Figs. 3(a)–3(c)] where the pressures calculated from different simulation methods are relatively consistent. Figure 3(d) shows that the theoretical results are between two sets of simulation data. Because of the free energy barrier, isotropic-nematic phase transition is difficult to identify by direct simulations. For example, no liquid-crystal phase was observed in the simulation for the system with only $m_r=8$ rigid segments at the packing fraction up to 0.479 but the theory predicts an I-N transition in the range of packing density $\eta=0.415-0.421$. In agreement with the theoretical predictions, similar phase transitions have been reported by Diplock *et al.*[45] for the case $m_r=8$ but at slightly higher packing densities ($\eta=0.446-0.453$).

The orientational order parameter provides a quantitative characterization of the orientational ordering in liquid-crystal systems. As for a rodlike system, the order parameter in a system of semiflexible chains is defined as

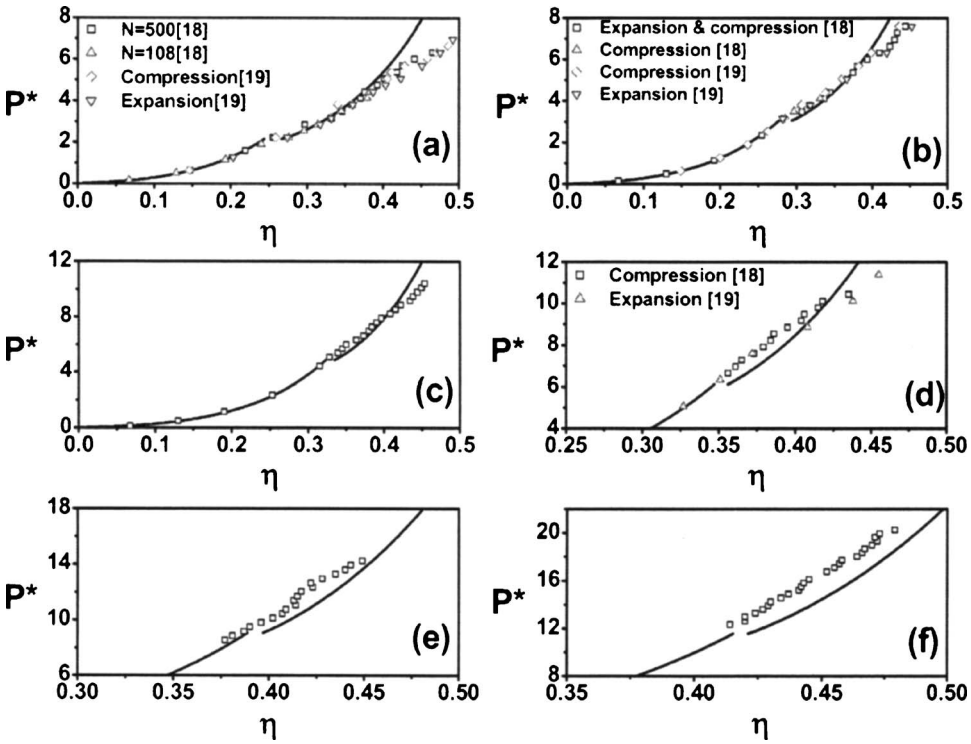

FIG. 3. Reduced osmotic pressure $P^*=\beta P\nu$ vs the packing density for rod-coil copolymers ($m=15$, $L=0.6\sigma$) with m_r=(a) 15, (b) 13, (c) 11, (d) 10, (e) 9, and (f) 8. The lines are theoretical predictions and the symbols are simulation results (Refs. 18 and 19).

$$S_2=\frac{1}{2}\int [3\cos^2(\Omega)-1]f(\Omega)d\Omega. \tag{15}$$

The value of the order parameter may vary from 0 in an isotropic phase to 1 in a nematic phase where the molecules are aligned perfectly parallel. Due to the cylindrical symmetry, $f(\Omega)$ can be reduced to a one dimensional function $f(\theta)$, where θ is the angle between the molecular axis and local director within the range of $[0,\pi/2]$. In the isotropic phase, the molecules are randomly oriented so that the system has a uniform orientational distribution $f(\theta)=1/4\pi$. Because the orientational distribution function is exactly known, we do not need to solve $f(\theta)$ for the isotropic phase. In the nematic phase, however, $f(\theta)$ must be solved by minimizing the Helmholtz energy at each packing fraction.

Figure 4 presents the orientational distribution functions at the melting points of the nematic phases shown in Fig. 3. For all cases $f(\theta)$ exhibits an exponential decay with the increase of θ as assumed *a priori* in some previous theoretical investigations.[51,52] An analytical approximation for $f(\theta)$ minimizes the computational effort and is useful especially for dealing with smectic phases that entail both orientational and spatial inhomogeneities.[5] However, the errors introduced by this simplification are sometimes not negligible.[8] Figure 4 shows that in all cases $f(\theta)$ peaks at the parallel direction, implying that the most favorable configuration is when most molecules are aligned parallel in the nematic phase. As expected, the alignment becomes more perfect when the molecular rigidity increases and the system containing rigid molecules ($m_r=15$) shows the highest distribution at the parallel direction.

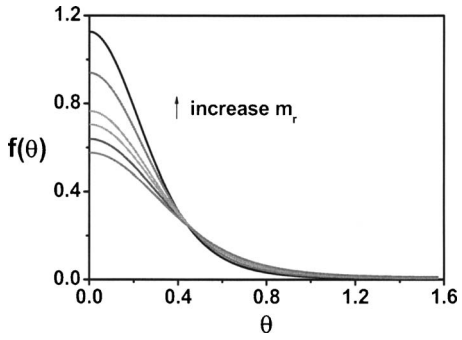

FIG. 4. Orientational distributions at the melting point of the nematic phase for the systems shown in Fig. 3.

Figure 5 compares the order parameters predicted from the theory with the simulation results. In the theoretical calculations, the order parameter in the isotropic phase is not considered. As a result, its value jumps from 0 in the isotropic phase to a positive value in the nematic phase. The Monte Carlo simulation gives a small value of the order parameter even in the isotropic phase. For systems containing rigid molecules (i.e., $m_r=15$ and 13), the theory finds a perfect agreement with the simulation results. It captures quantitatively the increase of the order parameters with the packing density. However, deviations are observed at low packing fractions probably due to the thermal fluctuations. For more flexible chains, the deviation of the theory from simulations is probably to inaccuracy of simulation results on the one hand and due to approximations introduced in the SPT on the other. The SPT may underestimate the coexisting densities at the I-N transition. As mentioned earlier, the simulation shows no nematic phase at $m_r=8$.

The I-N transition in lyotropic liquid crystals is usually known as an entropy-driven phase transition.[53] The origin of this transition comes from the competition of two types of entropy: the orientational entropy and the packing entropy, as defined in Eqs. (7) and (8), respectively. To quantify the in-

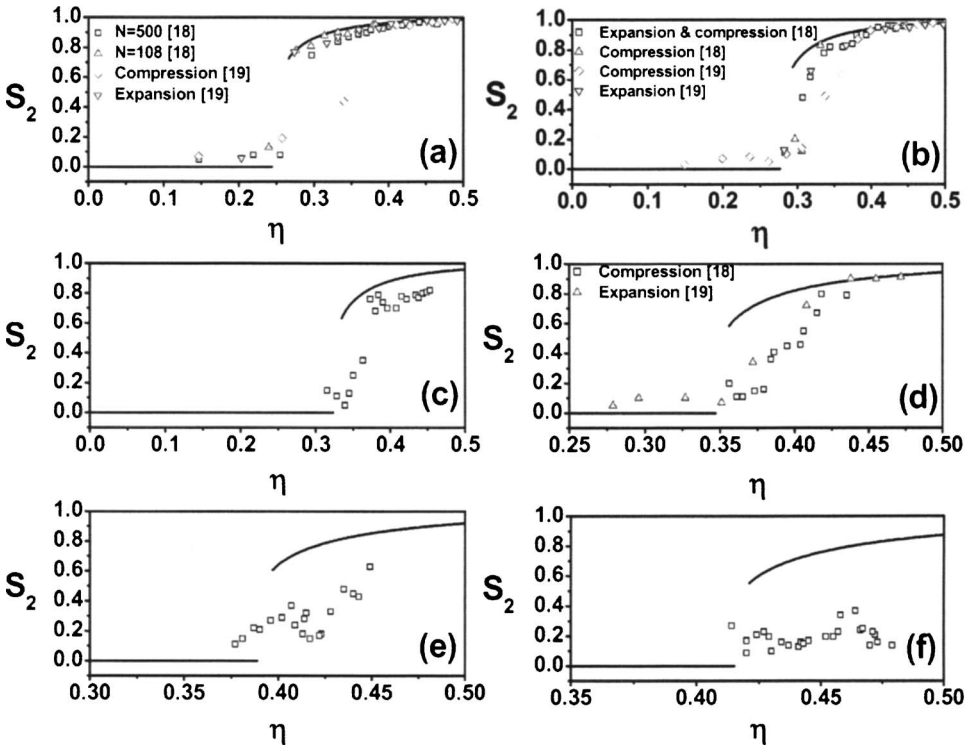

FIG. 5. Order parameter vs packing fraction for the same systems shown in Fig. 3. The lines are theoretical predictions and the symbols are simulation results (Refs. 18 and 19).

fluence of the chain flexibility on the competition of entropies, we calculate both orientational and packing entropies for rigid chains ($m_r=15$) and for those with a long flexible tail ($m_r=8$). Figure 6(a) shows that in both cases, the orientational entropy in a nematic phase is negative relative to that in an isotropic phase and the deviation increases with the packing density. The orientational entropy favors the random orientations or stabilizes the isotropic phase. However, the trend is different for the packing entropy. As shown in Fig. 6(b), at sufficiently high density the packing entropy favors the nematic phase and the gap between the packing entropy of the isotropic phase and that of the nematic phase widens as the polymer chains become more rigid. A combination of these two opposite effects on the entropy is responsible for the I-N phase transition in rod-coil copolymers. In comparison with that for rigid chains, the semiflexible chains have lower entropy penalty in orientational ordering and smaller gap between isotropic and nematic packing entropies. In other words, the chain rigidity plays a more significant role in stabilizing the nematic phase. As the chain rigidity increases, the nematic phase appears at a smaller packing fraction.

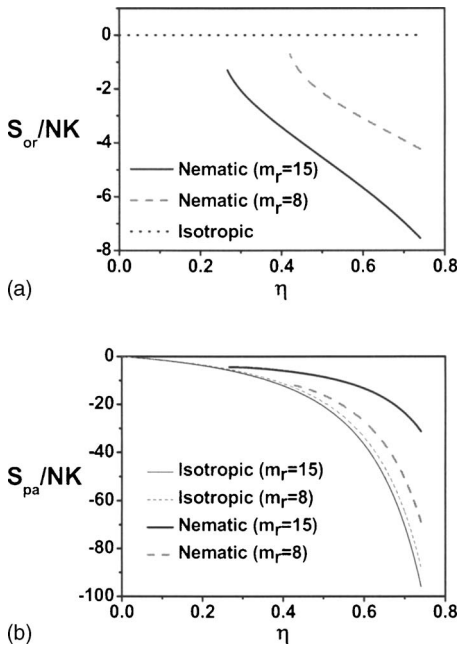

FIG. 6. The (a) orientational entropy and (b) packing entropy for rod-coil copolymers ($m=15$, $L=0.6\sigma$) with $m_r=15$ and 8.

B. Phase diagrams

1. Effect of the bond length

Until now the bond length is fixed at $L=0.6\sigma$ for direct comparison with the simulations. For a totally rigid chain, the change of the bond length is equivalent to the change in the molecular aspect ratio, which will lead to a shift of the coexisting packing densities at the I-N transition toward lower values. While the effect of bond length is well understood for rigid chains such as within the hard rod model or the hard spherocylinder model,[7] the trend is less obvious for rod-coil copolymers because an increase in the bond length results in changes in both the rigid and flexible components. For rigid chains, an increase of the aspect ratio, i.e., higher ratio of the chain length to width, tends to favor appearance of the nematic phase. For rod-coil copolymers, however, an increase of the bond length also raises the degree of freedom for the flexible block. For example, for a fused chain with the bond length $L=0.6\sigma$, the minimum bond angle is 112.89° while for a tangentially connected chain ($L=\sigma$), the mini-

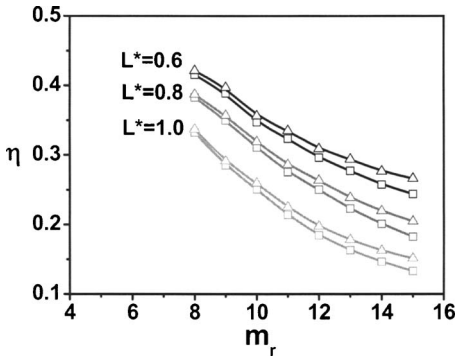

FIG. 7. Phase diagrams for the rod-coil copolymers ($m=15$) with bond lengths $L=0.6\sigma$, 0.8σ, and σ. The squares represent the coexisting isotropic packing fraction and the triangles represent the nematic packing fraction.

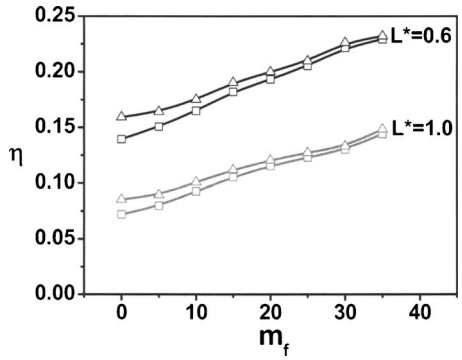

FIG. 8. Phase diagrams for the rod-coil copolymers with fixed length of the rigid block ($m_r=30$). The bond lengths covered are $L=0.6\sigma$ and σ. The different symbols have the same meaning as those in Fig. 7.

mum bond angle is 60°. The increase of the bond length thus introduces more flexibility in the coil block, which hinders the formation of the nematic phase.

Figure 7 shows the phase diagrams of rod-coil copolymers with different compositions and three different bond lengths $L=0.6\sigma$, 0.8σ, and σ. Here the total chain length remains fixed at $m=15$. The squares and triangles represent the coexisting packing fractions for the isotropic and nematic phases, respectively. As m_r decreases, the I-N transition shifts to higher packing fractions because the chain flexibility destabilizes the nematic phase. As the copolymers become more flexible, the coexisting densities become closer and the melting and freezing lines converge for $m_r<8$. Interestingly, it appears that the nematic phase ceases to exist when $m_r<8$, independent of the bond length. Our calculation suggests that the change of bond length has little effect on the minimum length of the rigid block necessary for the formation of the nematic phase.

As mentioned earlier, the increase of the bond length introduces two coupled effects: the increase in the aspect ratio of the rigid block and the increase in the flexibility of the coil block. Figure 7 shows that for all cases, the increase of the bond length reduces the packing fraction necessary for the I-N phase transition. It appears that the bond length has more prominent effect on the rigid block than on the flexible block. Because there are only few previous studies on the fused-chain model of liquid crystals, we are not aware of any systematical work on the effect of the bond length on I-N phase transition in rod-coil copolymers.

2. Effect of flexible tails

Another way to examine the effect of chain flexibility on the I-N phase transition is by adding a flexible tail to a rigid chain with fixed length. In an earlier simulation, McBride *et al.*[18] investigated such effect by comparing the results for two liquid-crystal models: a totally rigid chain ($m_r=11$, $m_f=0$) and a rod-coil chain ($m_r=11$, $m_f=4$). They found that addition of the flexible tail shifts the I-N transition to higher densities and thus destabilizes the nematic phase. However, it is not clear whether the nematic phase will disappear simply by increasing the length of the flexible tail. To address this question, we calculated the phase diagrams for rod-coil copolymers with the number of segments for the rigid block fixed at $m_r=30$. Figure 8 shows the results for two different bond lengths $L=0.6\sigma$ and σ. In both cases, addition of the coil block destabilizes the nematic phase, as observed in the molecular simulations. The trend is similar to that due to the change of the chain flexibility by adjusting the rod-coil composition. As the length of the flexible block increases, the I-N phase transition is shifted towards higher packing fractions. Interestingly, the nematic phase ceases to exist when the chain length for the flexible block is larger than $m_f=35$ for both the tangentially connected chains and fused chains. This result is quite unexpected because as we indicated earlier, the flexibility of the coil blocks is very different for the fused chain and for the tangent chain. This result affirms that the bond length has negligible effect on the minimum chain rigidity necessary for the formation of the nematic phase. On the minimum composition of the rigid block on the I-N transition, the prediction from the current work agrees well with the observation from a recent experiment.[24] For a series of rod-coil copolymers composed of poly (*p*-phenylene terephthalamide) (PPTA) and polyamide 6,6 (PA 6,6) blocks in the sulfuric solutions, it was found that the mole fraction of rigid PPTA block is at least 0.5 for the concentrated solutions to show a liquid-crystalline phase. With the length of PPTA fixed, the minimum concentration for the formation of a liquid-crystalline phase increases with the length of the flexible PA 6,6 block.

IV. CONCLUSIONS

We proposed a hybrid method for predicting the isotropic to nematic phase transitions for rod-coil copolymers by combing SPT with two-chain Monte Carlo simulations. While the former is accurate for the excluded volume effect, the latter describes faithfully the osmotic second virial coefficient for polymers of arbitrary topology. In comparison with a conventional equation of state, there are at least three key advantages of the proposed method. First, the two-chain simulation enables us to represent the osmotic second virial coefficient of semiflexible chains exactly. It avoids unnecessary errors introduced in analytical simplifications and correctly accounts for the effect of the chain flexibility even for the isotropic phase.[18] In addition, the new method is applicable to polymers of arbitrary architectures ranging from flexible, semiflexible, to rigid. With a proper generalization

of the Helmholtz energy, the new method can be further employed to deal with phase transitions with more complicated phases and inhomogeneous systems. Furthermore, it avoids the time-consuming ensemble average of chain configurations in the stage of solving the coexisting densities as required in alternative methods.[12,13]

The hybrid method predicts the osmotic pressures and order parameters for rod-coil copolymers ($m=15$, $L=0.6\sigma$) in good agreement with the simulation data. The numerical performance is satisfactory especially for systems with rigid chain configurations. We analyzed the effect of chain flexibility on the competition of orientational and packing entropies for the isotropic-nematic phase transitions and found that the packing effect becomes more significant as the rigidity of polymer chains increases. As hypothesized in previous theoretical works, the orientational distribution function exhibits an exponential decay from the maximum at the parallel direction to close to zero at the perpendicular direction. A comparison of the orientational entropy and the packing entropy between the isotropic and nematic phases explains quantitatively the driving force for the I-N phase transition. Because of the dominance of the orientational entropy, the isotropic phase is stable at low packing fractions. At high packing fractions, the system gains packing entropy by transferring into the nematic phase.

We have also investigated the effects of the bond length and the tail length on the structural ordering in rod-coil copolymers. A decrease of the length ratio between the rigid block m_r and the flexible block m_f results in higher coexisting packing fractions at the I-N transition and subsequently the gap between the coexisting densities diminishes. While an increase of the bond length induces two opposite effects on the phase transition by raising the polymer aspect ratio and the flexibility of the coil block, it appears that the orientational effect dominates and the minimum packing fraction necessary for the nematic phase is reduced as the bond length increases.

The flexibility of a polymer chain can also be altered by adding a flexible tail to a rigid block. According to the calculated phase diagrams for fused and tangent chains with fixed number of segments in the rigid block ($m_r=30$), we found that addition of a flexible tail hinders formation of the nematic phase and the trend is similar for tangent and fused chains, even though they have very different flexibilities. The nematic phase ceases to exist when the flexible tail length exceeds $m_f=35$, independent of the bond length. This prediction finds excellent agreements with the recent experiments on PPTA with PA 6,6 block copolymers.

ACKNOWLEDGMENTS

The authors are grateful to Dr. Toshi Hino for useful discussions. This research is supported by the U.S. Department of Energy (DE-FG02-06ER46296) and used resources of the National Energy Research scientific Computing Center, which is supported by the Office of Science of the U.S. Department of Energy under Contract No. DE-AC03-76SF00098.

[1] L. Onsager, Ann. N.Y. Acad. Sci. **51**, 627 (1949).
[2] F. C. Bawden, N. W. Pirie, J. D. Bernal, and I. Fankuchen, Nature (London) **138**, 1051 (1936).
[3] P. J. Flory, Proceedings of the Royal Society of London Series a-Mathematical and Physical Sciences 234, 73 (1956).
[4] A. R. Khokhlov and A. N. Semenov, Physica A **108**, 546 (1981).
[5] A. R. Khokhlov and A. N. Semenov, Physica A **112**, 605 (1982).
[6] J. D. Parsons, Phys. Rev. A **19**, 1225 (1979).
[7] S. D. Lee, J. Chem. Phys. **87**, 4972 (1987).
[8] S. D. Lee and R. B. Meyer, J. Chem. Phys. **84**, 3443 (1986).
[9] C. Vega and S. Lago, J. Chem. Phys. **100**, 6727 (1994).
[10] D. C. Williamson and G. Jackson, J. Chem. Phys. **108**, 10294 (1998).
[11] H. Fynewever and A. Yethiraj, J. Chem. Phys. **108**, 1636 (1998).
[12] K. M. Jaffer, S. B. Opps, D. E. Sullivan, B. G. Nickel, and L. Mederos, J. Chem. Phys. **114**, 3314 (2001).
[13] K. M. Jaffer, S. B. Opps, and D. E. Sullivan, J. Chem. Phys. **110**, 11630 (1999).
[14] P. Bryk and R. Roth, Phys. Rev. E **71**, 011510 (2005).
[15] D. Frenkel and B. M. Mulder, Mol. Phys. **55**, 1171 (1985).
[16] C. Vega, C. McBride, and L. G. MacDowell, J. Chem. Phys. **115**, 4203 (2001).
[17] A. Yethiraj and H. Fynewever, Mol. Phys. **93**, 693 (1998).
[18] C. McBride, C. Vega, and L. G. MacDowell, Phys. Rev. E **64**, 011703 (2001).
[19] C. McBride and C. Vega, J. Chem. Phys. **117**, 10370 (2002).
[20] J. W. Park and E. L. Thomas, Adv. Mater. (Weinheim, Ger.) **15**, 585 (2003).
[21] B. D. Olsen and R. A. Segalman, Macromolecules **38**, 10127 (2005).
[22] B. D. Olsen and R. A. Segalman, Macromolecules **39**, 7078 (2006).
[23] K. Van De Wetering, C. Brochon, C. Ngov, and G. Hadziioannou, Macromolecules **39**, 4289 (2006).
[24] C. de Ruijter, W. F. Jager, L. B. Li, and S. J. Picken, Macromolecules **39**, 4411 (2006).
[25] C. de Ruijter, W. F. Jager, J. Groenewold, and S. J. Picken, Macromolecules **39**, 3824 (2006).
[26] T. W. Schleuss, R. Abbel, M. Gross, D. Schollmeyer, H. Frey, M. Maskos, R. Berger, and A. F. M. Kilbinger, Angew. Chem., Int. Ed. **45**, 2969 (2006).
[27] K. K. Tenneti, X. F. Chen, C. Y. Li, Y. F. Tu, X. H. Wan, Q. F. Zhou, I. Sics, and B. S. Hsiao, J. Am. Chem. Soc. **127**, 15481 (2005).
[28] S. Lu, T. X. Liu, L. Ke, D. G. Ma, S. J. Chua, and W. Huang, Macromolecules **38**, 8494 (2005).
[29] T. Sarbu, T. Styranec, and E. J. Beckman, Nature (London) **405**, 165 (2000).
[30] G. Yu, J. Gao, J. C. Hummelen, F. Wudl, and A. J. Heeger, Science **270**, 1789 (1995).
[31] E. A. Minich, A. P. Nowak, T. J. Deming, and D. J. Pochan, Polymer **45**, 1951 (2004).
[32] M. W. Matsen and C. Barrett, J. Chem. Phys. **109**, 4108 (1998).
[33] D. Duchs and D. E. Sullivan, J. Phys.: Condens. Matter **14**, 12189 (2002).
[34] V. Pryamitsyn and V. Ganesan, J. Chem. Phys. **120**, 5824 (2004).
[35] C. L. Chochos, P. K. Tsolakis, V. G. Gregoriou, and J. K. Kallitsis, Macromolecules **37**, 2502 (2004).
[36] C. McBride and M. R. Wilson, Mol. Phys. **97**, 511 (1999).
[37] J. S. van Duijneveldt and M. P. Allen, Mol. Phys. **92**, 855 (1997).
[38] T. Hino and J. M. Prausnitz, Polymer **40**, 1241 (1999).
[39] D. C. Williamson and G. Jackson, Mol. Phys. **86**, 819 (1995).
[40] T. Boublik, Mol. Phys. **68**, 191 (1989).
[41] T. Boublik, C. Vega, and M. Diazpena, J. Chem. Phys. **93**, 730 (1990).
[42] T. Boublik, J. Chem. Phys. **63**, 4084 (1975).
[43] T. Boublik and I. Nezbeda, Chem. Phys. Lett. **46**, 315 (1977).
[44] M. A. Cotter, J. Chem. Phys. **66**, 1098 (1977).
[45] R. Diplock, D. E. Sullivan, K. M. Jaffer, and S. B. Opps, Phys. Rev. E **69**, 062701 (2004).
[46] F. J. M. Hoeben, P. Jonkheijm, E. W. Meijer, and A. Schenning, Chem. Rev. (Washington, D.C.) **105**, 1491 (2005).
[47] H. P. William, A. T. Saul, W. T. V., and P. F. Brian, *Numerical Recipes in FORTRAN 77: The Art of Scientific Computing* (Cambridge University Press, Cambridge, 1992).
[48] J. Herzfeld, A. E. Berger, and J. W. Wingate, Macromolecules **17**, 1718

(1984).
[49] A. Yethiraj, J. Chem. Phys. **101**, 9104 (1994).
[50] C. Vega, Mol. Phys. **98**, 973 (2000).
[51] G. Cinacchi, L. Mederos, and E. Velasco, J. Chem. Phys. **121**, 3854 (2004).
[52] J. P. Straley, Phys. Rev. A **8**, 2181 (1973).
[53] G. J. Vroege and H. N. W. Lekkerkerker, Rep. Prog. Phys. **55**, 1241 (1992).